Wiley
Geofluids
Volume 2024, Article ID 2183265, 17 pages
https://doi.org/10.1155/2024/2183265

WILEY

Research Article

Fine Characterization of Nonmain Oil Layer Distributions in Complex Fault Block Oilfield and Its Development Model

Lei Xu,[1] **Xiutian Yao**,[1,2] **Sen Yan**,[1] **Zhang Wen**,[1] **and Jimei Xue**[1]

[1]*Gudao Oil Recovery Plant, Shengli Oilfield Company, SINOPEC, Dongying 257231, China*
[2]*School of Energy Resources, China University of Geoscience, Beijing 100083, China*

Correspondence should be addressed to Xiutian Yao; yxiutian@163.com

Received 22 January 2024; Revised 30 April 2024; Accepted 7 May 2024; Published 30 May 2024

Academic Editor: Azizollah Khormali

Improving the oil production from nonmain oil layers is crucial for the complex fault block oilfields during the late stage of high water cut development to ensure stable production and capacity expansion. However, the developing characterization of the nonmain layers and their remaining oil distribution is still inadequate. Developing an efficient mode of development remains a challenge. This paper presents a detailed characterization of the sedimentary microfacies and architecture of a nonmain reservoir based on core and logging data analysis. A flexible injection-production development strategy model was designed and applied in the Hetan oilfield, located in the southeast of Zhanhua Depression of Bohai Bay Basin as an example. The results show that the nonmain oil layer of the Hetan oilfield is composed of estuary bar microfacies sand bodies. Deposits of various shapes are formed on the side or in front of the main body of the estuary dam, which constitutes the nonmain oil reservoir. The lithology is fine, the sand body thickness is small, and the plane heterogeneity is strong. The distribution is banded, potato-shaped, and fragmented. The nonmain oil layer has a small oil-bearing area of 0.1-1.0 km^2 and a high oil saturation of over 58%. The Hetan oilfield has a significant amount of remaining oil enrichment and considerable potential for production digging. To optimize production, a flexible injection and production adjustment scheme is proposed, which includes designing multitarget horizontal wells and utilizing various methods such as optimizing well spacing, coupled injection, and cycle injection. Field tests conducted in the area have shown an increase in the recovery factor of nonmain oil layers from 16.7% to 28.5%. This indicates that identifying and characterizing nonmain oil layers through detailed analysis of sedimentary microfacies and reservoir architecture is useful in the late-stage development of complex fault block reservoirs to maintain sustainable and efficient oilfield development.

1. Introduction

During the late stage of high water cut in complex fault-block oilfield development, the distribution of remaining oil becomes increasingly complex and dispersed in space, making development more challenging [1, 2]. The multilayer property and heterogeneity of the reservoir, as well as the complexity of the well pattern, have made the distribution of oil and water in the reservoirs more complex, resulting in a more dispersed, fragmented, or fractured remaining oil reserve [1, 3]. The well pattern demonstrates a high level of control over the main oil reservoirs, with a high degree of reserve utilization and a high integrated water cut. In contrast, the well pattern for the nonmain reservoirs has less adjustment, resulting in a relatively low degree of control over the well pattern and poor reserve utilization [4]. Although the nonmain oil layer still contains a significant amount of oil with high saturation, the main oil reservoir experiences serious water breakthroughs in the later stages of development, leading to a rapid decline in production [5, 6]. Nonmain reservoirs are a relative concept characterized by geological features such as being small, scattered, thin, and poor in comparison to the main reservoir in a complex fault block oilfield [4]. To improve the development of nonmain reservoirs, previous authors conducted microstructure, sediment microphase, and architecture element analyses to study the development characteristics of various nonmain reservoirs [7]. The detailed description of the

reservoir is based on an analysis of the remaining oil control factors. Supporting and adjusting technologies, such as hydraulic fracturing and the dominant direction of the injection well, have significantly improved the injection-production relationship of a single sand body in a nonmain reservoir, resulting in increased recoverable reserves and improved development effects [8–10].

The Hetan oilfield is a typical small fault-block oilfield located in the Zhanhua sag of the Bohai Bay Basin in northern China [11]. The main oil layer of the field is facing several issues, including high water cuts, scattered distribution of remaining oil, poor utilization of water-flooding reserves, and prominent injection-production contradictions. The remaining oil in the nonmain oil layer is generally enriched and has relatively high oil saturation [12]. The efficient development of the Hetan oilfield greatly depends on the reasonable potential digging development of the nonmain reservoir. However, the nonmain oil layer still lacks sufficient control over the well pattern, resulting in large uncontrolled oil reserves. Furthermore, the effective well spacing is less than 500 m, and the well pattern is poorly suited for the area. Therefore, further research is necessary to identify the characteristics and mode of development for the nonmain oil layer. This study focuses on the distribution characteristics and development mode of the nonmain reservoir of the field. Core, deposition, and logging data will be used to analyze the sedimentary microfacies and architecture of the reservoir in order to characterize reservoir quality and remaining oil distribution. Furthermore, injection and production methods will be optimized. The results have significantly improved the effectiveness of reservoir development.

2. Geological Setting

2.1. Reservoir Geology. The Hetan oil field is tectonically developed in the Gunan sub-sag eastern part of the Zhanhua sag in the Jiyang depression, Bohai Bay Basin, northern China, separated from the Fulin sub-sag in the south by a central fault zone (Figure 1(a)) [12]. The field is a reverse ridge-type fault block reservoir that is controlled by the Kenbei fault zone (Figure 1(b)). The stratum structure is generally high in the south and low in the north, with a stratigraphic dip of 8-10°. The highest point of the structure is located near the GN24-76 well, which has a vertical inheritance and a consistent structure pattern. The oilfield structure is mainly influenced by the northeast, northern, and eastern faults. The block is relatively intact and independent, with two sets of subfaults developing internally parallel to the main fault, making the block relatively closed.

The oil-bearing formation in the Hetan oilfield is the Shahejie Formation, which can be divided into three sections named S3, S2, and S1 from bottom to top (Figure 2). The S3 consists of sandy mudstone interbedded deposits with a thickness of 140-230 m. The reservoir lithology is siltstone interbedded with conglomerate sandstone and gray dolomite. The thickness of the oil layer varies greatly from 6 to 39 m, and the sorting coefficient ranges from 1.27 to 1.58. The reservoir has an average porosity of 28.9% and an average permeability of $2153 \times 10^{-3}\ \mu m^2$. The mud content ranges from 4% to 8%, and the cementation type is contact to pore type with the calcareous mud cementation. The S2 consists of interbedded sandstones and mudstones. The reservoir is dominated by conglomeratic sandstones and siltstones interbedded with gray sandstones. The distribution of sandstone is stable, with a thickness of 110-116 m. The oil layer thickness ranges from 12.8 to 34.4 m. The sorting coefficient is 1.17-2.85. The cementation is mud-calcareous, with a contact-pore type and a basal-pore type. The mud content is 8%, and the average porosity is 28.9%. The average air permeability is $1{,}880 \times 10^{-3}\ \mu m^2$. The S1 consists of biological limestone, dolomite, and calcareous sandstone, with a thickness ranging from 70 to 95 m. The depositional environment of S2 and S3 consists of near-source river delta deposits (Figure 3). These deposits belong to the delta front subphase and develop submerged diversion waterway microphase and estuary dam microphase deposits. They have rich source types and diverse reservoir sand bodies, mainly medium and fine sandstones, with well-developed pore space and good reservoir permeability properties. The oil has low density and viscosity, resulting in a large reserve abundance (420×10^4 t/km^2). This is a typical example of a "small and fat" block oil reservoir [11]. The Hetan oilfield consists of stratified oil reservoirs, comprising 44 small oil layers from S1 to S3. Each layer has an inconsistent oil-water boundary and a complex oil-water relationship. The oil-bearing area gradually decreases from top to bottom.

2.2. Oilfield Development Condition. The Hetan oilfield underwent development in 1987 and was initially highly productive. However, the strong injection and production approach resulted in a short period of water-free oil production and a rapid rise in water cut for the field as a whole. After one year of production, the water cut rose quickly and production continued to decline [12]. The Hetan oilfield was initially developed from three sets of development reservoirs: S2-1, S2-2, and S3. The average well spacing in the field was 350 meters, as illustrated in Figure 4, which shows the well pattern in the S2-1 developing layer as an example. The average daily oil production per well was 87.5 t. The layer S2 had an average of 80 t/day, while the S3 layer had an average of 103 t/day. The maximum oil production rate reached 5.49% (note: the oil production rate is the percentage of actual oil production per year in relation to the geological reserves or recoverable reserves of the field, which is a key parameter of the development level of oil fields used in China). During the initial development stage from 1987 to 1993, the average oil production rate was 4.0%. However, the annual decline rate was higher, reaching 35.4%. In 1993, the reservoir development system was adjusted to four sets by subdividing S2-2 into S2-$2^{1\text{-}4}$ and S2-$2^{5\text{-}7}$. The injection and production methods were strongly adjusted by implementing unstable water injection, and the well pattern was encrypted to produce the remaining oil and increase the degree of reserve utilization. The oil production rate initially reached 4.6% but gradually declined in later stages, with the final rate being only 0.43%. In recent years, the Hetan oilfield has further implemented measures to adjust the injection and production structure and improve comprehensive

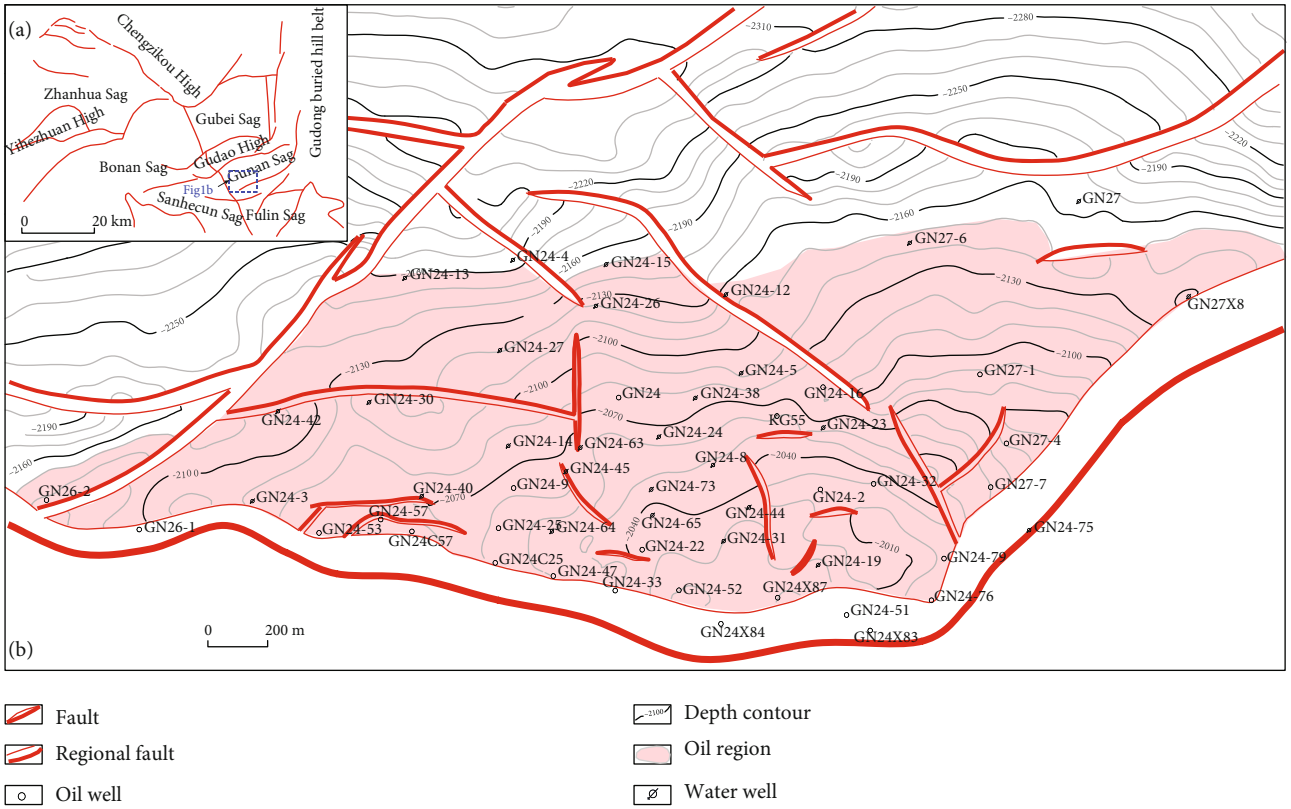

FIGURE 1: Structural map of the Hetan oilfield. (a) The regional structural setting and location of the study area in the Zhanhua Depression of Bohai Bay Basin, northern China. (b) The structural isoline, faults, oil-bearing area, and well pattern on the top structural map of the S2-2 reservoir of the Hetan oilfield at present.

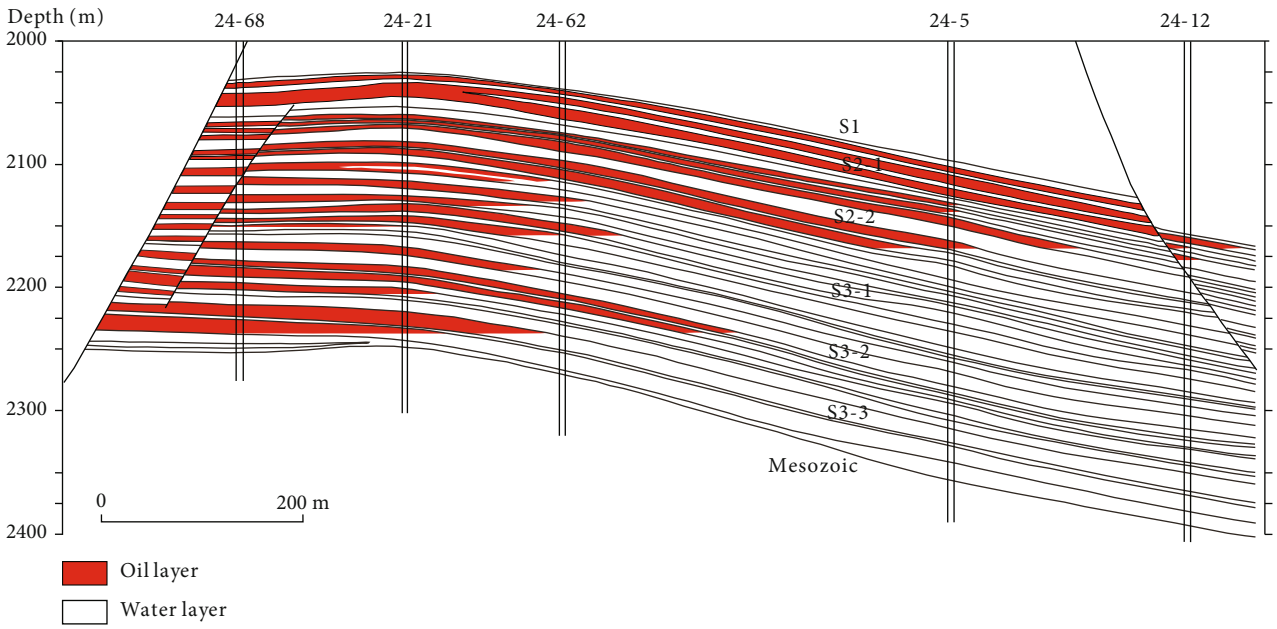

FIGURE 2: Reservoir geological profile of the Hetan oilfield in the south-north direction.

management. These measures include stratified water injection, subdivision and restructuring of the reservoir system, and interlayer replacement. As a result, the integrated oil production rate decline has been reduced to 2.3%, and the oil recovery factor has reached 52%, indicating positive development effectiveness. The Hetan oilfield is currently

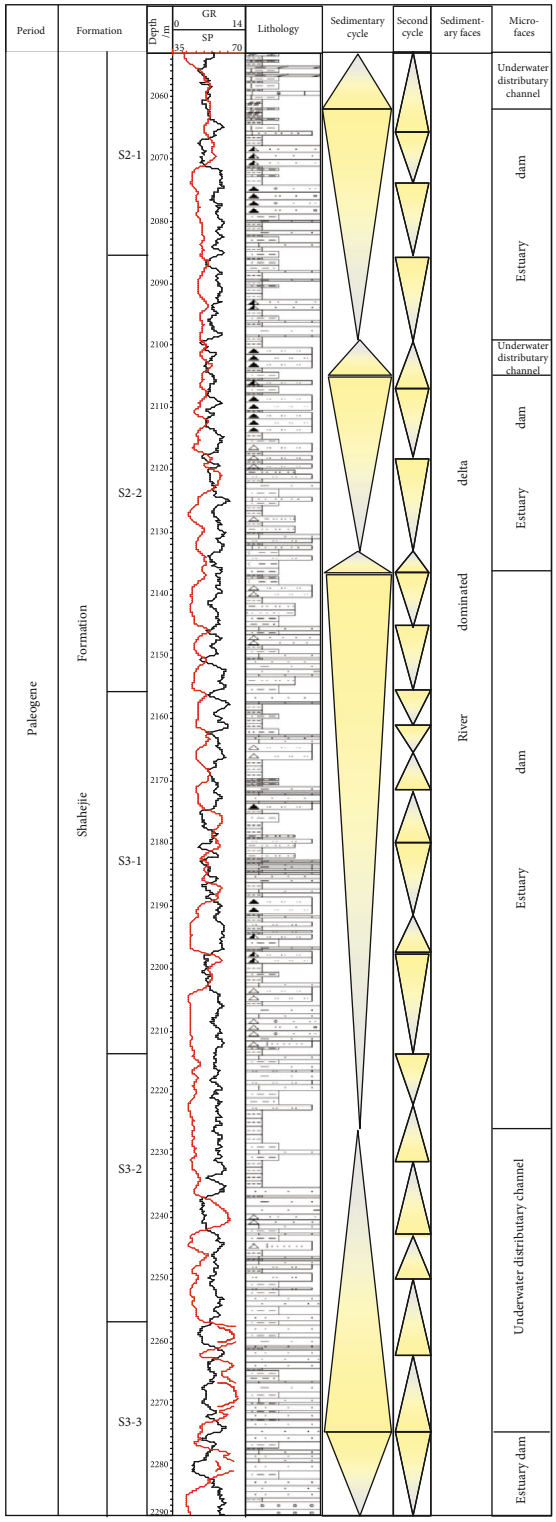

Figure 3: Comprehensive column chart of the main geological formation in the Hetan oilfield, displaying the gamma ray (GR) and spontaneous-potential (SP) log curves.

facing significant challenges due to infrequent water well operations, poor injection water quality, high start-up pressure (8.6 MPa), and a low water absorption index (4.2 m^3/(d·MPa)). These factors have led to a prominent contradiction between injection and production, which threatens the sustainable development of the Hetan oilfield.

3. Materials and Methods

This study employs sedimentary microfacies, architecture anatomy, and well pattern optimization to develop a methodology for identifying and developing remaining oil in nonmain reservoirs. The challenges of identifying and classifying nonmain oil reservoirs, as well as the distribution of remaining oil and the imperfections of injection-production well patterns, are addressed. This paper analyzes the oilfield drilling cores, spontaneous potential log (SP), resistivity log (R4), and conductivity log (COND), as well as the production data from the Hetan oilfield. The research process of this study consists of three main steps. First, we analyze the microfacies and architecture characteristics of the nonmain oil layer based on the sedimentary architecture principle and saturation logging interpretation. Next, we identify and divide the nonmain oil layers. The petrophysical properties and oil and water saturation characteristics of the nonmain oil layer were analyzed based on the core tests and logging data. Furthermore, the spatial and remaining oil distribution characteristics of the nonmain oil layer were defined. Finally, the technical limit well spacing calculation method was used to optimize the well pattern of nonmain oil layers. A development strategy for producing remaining oil from nonmain oil layers was proposed based on the existing well pattern. A field test was conducted in the study area to verify the potential development effect of nonmain oil layers.

4. Results

4.1. Fine Identification of Nonmain Oil Layers

4.1.1. Sedimentary Microfacies. The S2 and S3 of the Shahejie Formation in the Hetan oilfield are primarily sourced from the Chenjiazhuang high. The sedimentary environment is characterized by near-source fluvial deltaic deposition, which is a typical deltaic foreland subphase. The fine layer of gray mud shale in S3 is straight and parallel to the layer (Figure 5(a)) and continuous or intermittent. The S3 is a subface of the delta front that forms in a low-energy environment due to the continuous deposition of fine-grained sediments.

The middle and upper sectors of S3 are primarily composed of brown-yellow medium sandstone, fine sandstone, and brown-gray siltstone. These layers exhibit good particle sorting and fine-bedded mudstone, which often develop cross-bedding, wavy bedding, and scour and fill structures (Figures 5(b) and 5(c)). The fine layers within the strata are inclined and oblique to the plane or layer interface (Figure 5(d)), and fragments of plant fossils are visible (Figures 5(e) and 5(f)). The induction logging curve exhibits a toothed pattern, as shown in Figures 6(a) and 6(b), and is mainly composed of microfacies from the underwater distributary channel. The lower part of S3 consists mainly of gray and gray-white fine sandstone and siltstone with parallel, cross, and oblique bedding. The SP curve has a funnel

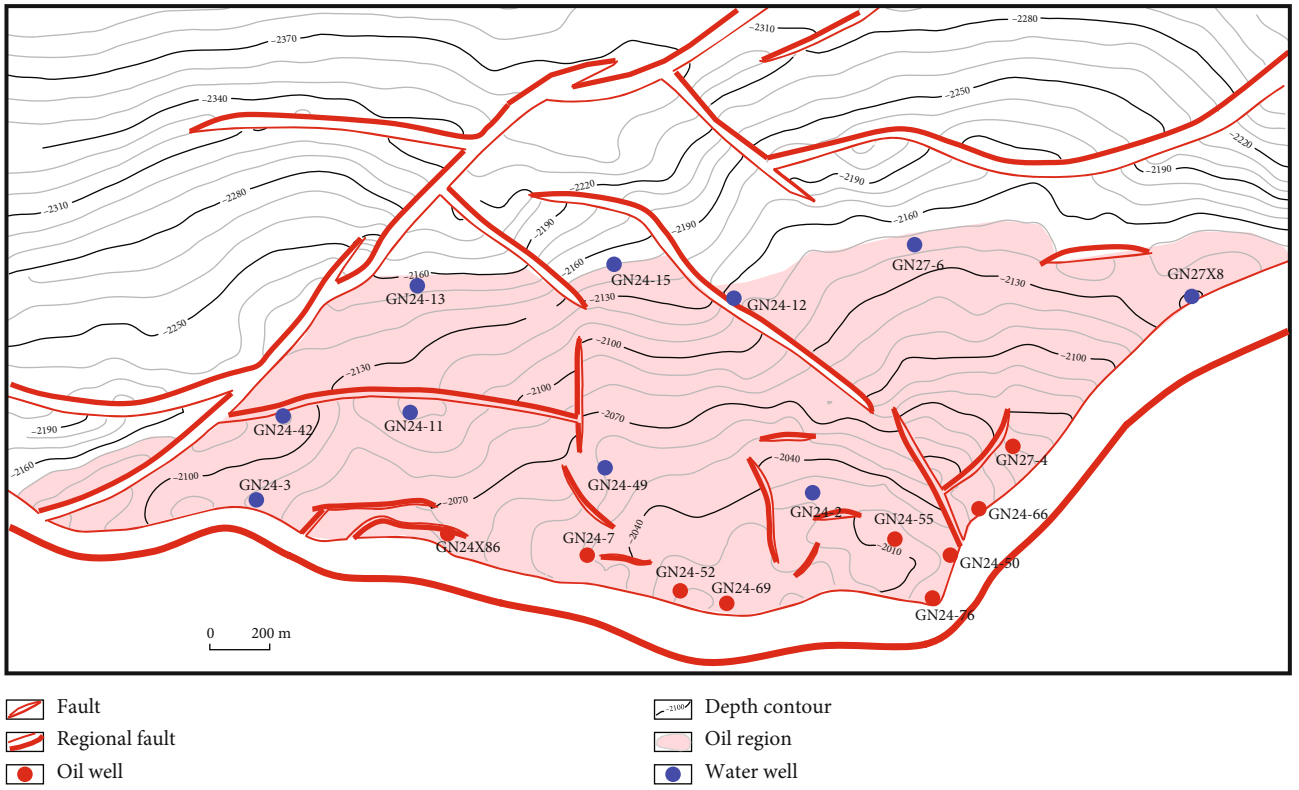

Figure 4: The injection and production well pattern for the S2-1 developing layer in the Hetan oilfield.

shape, and the COND curve in Figure 6(c) also shows a toothed pattern. The microfacies of the delta-front estuary bar are predominant.

The upper sector of S2 is primarily composed of gray-yellow pebbly sandstone and coarse sandstone (Figures 5(g) and 5(h)). The SP curve exhibits a box-shaped and tooth-shaped pattern, which indicates that the microfacies are characterized by an underwater distributary channel (Figure 6(d)). The lower sector of S2 is composed of brown-gray fine sandstone and siltstone. The sand layer is a medium-to-thick layer and mainly consists of well-sorted sand and silty sand with few fossils. Wedge cross-bedding, parallel bedding, and occasionally bioturbation structures are present, as well as local carbonaceous dust. The SP curve has a funnel shape, while the COND curve has a toothed shape (Figures 6(e) and 6(f)), which corresponds to the microfacies of the delta front estuary bar.

4.1.2. Sedimentary Architecture. The study area's fan delta frontal reservoir was divided into three graded interfaces vertically based on the principle of hierarchy in conformational studies. This was determined by analyzing the core data and logging data of the S2 reservoir's architectural interface. The interface between the five-grade and four-grade layers is composed of deltaic mud reservoirs located between estuarine dams or diverging channel complexes. The four-grade interface, on the other hand, is a petrophysical interlayer found between a single estuarine dam or a single submerged diverging channel. This interlayer is typically composed of mudstone or siltstone with poor petrophysical properties, and it can act as a barrier to internal seepage in the sand body. The three-grade interface acts as an interlayer between accretionary bodies within a single estuarine dam deposit. It is mainly composed of muddy siltstone with limited extension and thin thickness and generally acts as a local barrier to fluids or retards their flow. The estuarine dam near the underwater diversion channel is coarser in lithology and thicker in sand and constitutes the main body of the estuarine dam. The deposits on the edge of the estuarine dam have a different shape and are formed with finer lithology and smaller sand thickness on the side or front of the main body of the estuarine dam.

Based on the log curves of SP and COND logging, the estuarine dam deposit face in the study area can be further divided into two architectural elements: the main body of the dam and the edge of the dam (Figure 7). The main body of the dam consists mainly of fine sandstone and medium sandstone, with thicknesses of 3-8 m and exhibiting anticlinal characteristics. The reservoir is well-developed and serves as the main oil layer. On the other hand, the dam's edge is primarily composed of fine sandstone and siltstone, with thicknesses of 1-3 m and exhibiting either anticlinal or finger-like characteristics. The reservoir is poor and serves as the nonmain oil layer. By applying this method to other wells and sand formations in the study area, we can obtain the distribution characteristics of nonmain layers. This will allow us to evaluate the reservoir quality and remaining oil distribution.

4.1.3. Distribution of Nonmain Oil Layer. Using the fourth small oil layer of the S2-2 section (signed as S2-2^4) as an

(a) (b)

(c) (d)

(e) (f)

Figure 5: Continued.

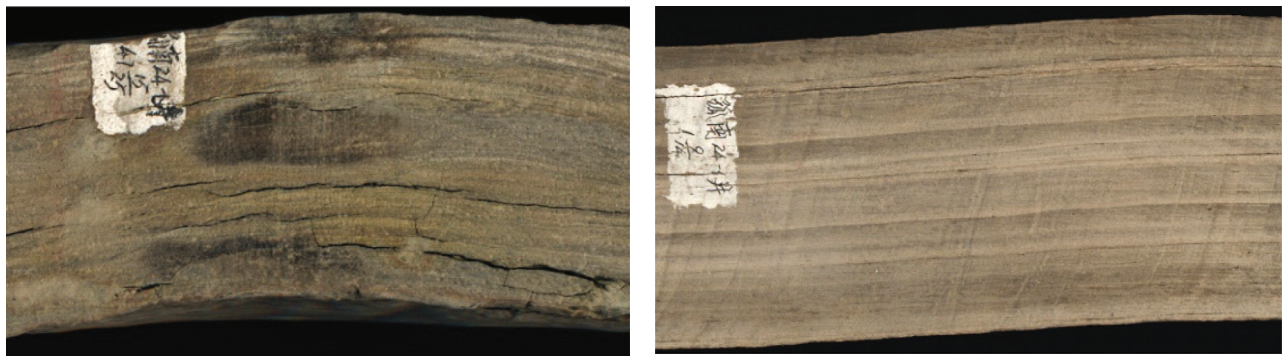

(g) (h)

Figure 5: Rock specimen photos of Shahejie Formation in Hetan oilfield. (a) Predelta mudstone interlayer. (b) Parallel bedding in fine sandstone. (c) Parallel bedding of medium sandstone. (d) Wave-built cross bedding. (e) Bioturbation structure. (f) Fragments of fossil plants. (g) Coarse sandstone parallel bedding. (h) Parallel bedding of medium-fine sandstone.

example, we first divided S2-2 vertically into a temporal stratigraphic framework of submerged diversion channels and estuarine dams based on the principle of sequence stratigraphy. We then identified the estuarine dams and divided them into the main body and the edge within the single reservoir framework (Figure 8). The main body of the estuary dam is primarily composed of fine sandstones, with a smaller proportion of medium sandstones and siltstones. Positive, uniform, and antigrain sequences are visible. Due to the location of sand body deposition, the grain sequence near the end of the distributary channel is positive, while the grain sequence near the front delta is reversed. The sand body's grain size probability curve is three-stage. At the bottom of the estuary dam, bioclasts, such as snails, are visible. The sedimentary structures present include parallel bedding, oblique bedding, and cross-bedding. The logging curves exhibit various shapes, such as bell, box, funnel-box, and trapezoid. The dam edge is characterized by fine grain size and thin thickness, with lithologies of fine sandstone and siltstone, and the development of parallel and undulating laminations. The shape of its logging curve can be described as funnel-shaped, tooth funnel-shaped, or spindle-shaped. The main body of the dam is separated from the dam edge by an unstable, muddy, or calcareous interlayer. Thus, the main oil reservoir of the estuarine dam microfacies, which was previously thought to be a single connected area, is actually a composite sand body consisting of multiple phases of the main body of the estuarine dam and the sand body of the dam edge stacked on top of each other in the longitudinal direction. Thin, stable, and muddy interlayers develop between them.

The distribution and contact relations of the nonmain oil layer on the plane can be more accurately described by combining the architectural elements. To characterize the distribution morphology of a single architectural layer on the plane, we analyzed the architectural elements in detail, using the nonmain oil reservoir of S2-2 as an example. The results indicate that the nonmain oil reservoirs in the edge face of the estuary dam exhibit a striped, potato-like, and fragmented plan due to the spreading of the sedimentary architectural element. These reservoirs display significant planar variation and strong heterogeneity. As shown in Figure 9, the S2-2^{11} and S2-2^{41} reservoirs are striped and fragmented, covering an area of less than 1 km^2 (Figures 9(a) and 9(b)). On the other hand, the S2-2^{51}, S2-2^{32}, and S2-2^{61} reservoirs are potato-shaped, with a local distribution and a smallest area of 0.1~0.3 km^2 (Figures 9(c) and 9(d)).

The main oil layers in the Hetan oilfield are primarily composed of sedimentary microfacies in underwater distributary channels and estuarine bars, as determined by lithology and electrical calibration. These layers have a wide development range, continuous distribution, large reservoir thickness, and small differences in physical properties in the plane. The sand thickness ranges from 3.2 to 6.5 m, with an average of 5.3 m, and shows little variation in plane. The porosity ranges from 15.1% to 33.2%, with an average of 26.5%. Physical properties are relatively uniform across planes. While the nonmain oil layers are primarily located in the interlayers or edges of estuarine dams and at the edges of lobes, the sand bodies are in contact with the main body of dams and lacustrine mud and exhibit strong planar heterogeneity. They are characterized by being small, scattered, thin, and poor, meaning that their development range is limited, their distribution is scattered, the thickness of the sand bodies is thin, and their physical properties are poor.

4.2. Reservoir Quality and Remaining Oil Distribution of Nonmain Formation

4.2.1. Reservoirs Petrophysical Differences. There are significant differences in sediment grain size, sorting, and mud content among different microfacies architectures in delta front reservoirs, indicating a strong planar petrophysical heterogeneity [13]. This paper determines the quality difference of the nonmain oil reservoir in the delta front estuary dam edge facies in the Hetan oilfield by combining core sampling analysis data and reservoir architecture anatomy based on the fine division of the nonmain oil layer architecture element. The results are listed in Table 1. The results show that the thickness of the sand body in the nonmain reservoir is generally between 1.0 and 3.0 m with a small area of 0.1 to 1.0 km^2. The porosity ranges from 10.0% to 30.0%,

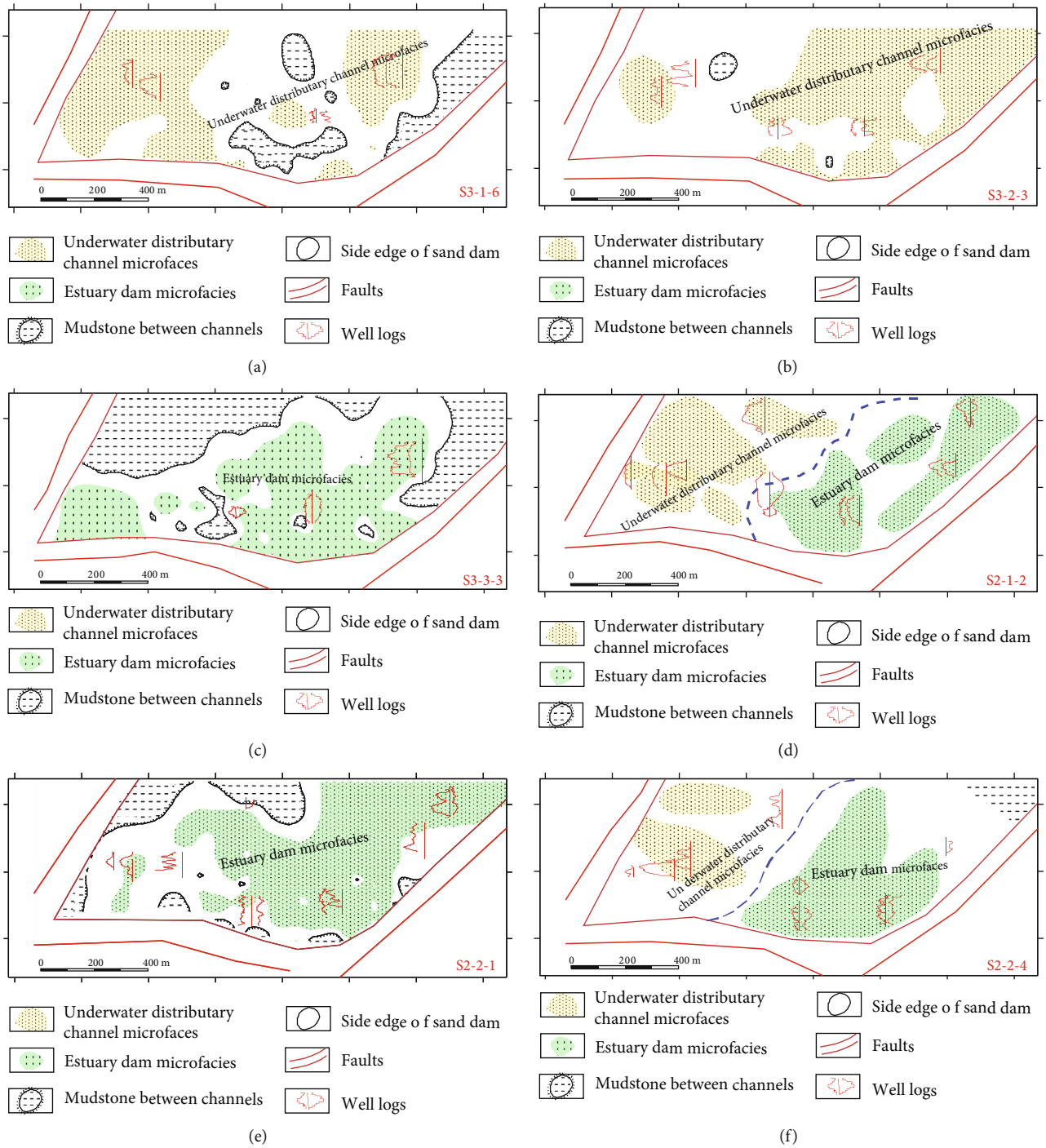

Figure 6: Maps of sedimentary microfacies of (a–c) S3 and (d–f) S2 in the Hetan oilfield. Logging curves for typical wells are also shown, with the SP curve on the left side of the well and COND on the right.

and the permeability ranges from 221×10^{-3} to $1054 \times 10^{-3}\ \mu m^2$. The reservoir has good porosity-permeability properties, belonging to a high-porosity and middle-permeability reservoir. However, there is strong heterogeneity in the permeability distribution within the plane, with coefficients of variation ranging from 0.71 to 0.9. The petrophysical properties of the nonmain layer exhibit significant changes due to the sedimentary architecture, resulting in strong heterogeneity. However, there is some regularity to this heterogeneity.

4.2.2. Potential Remaining Oil Distribution. The distribution of remaining oil is typically affected by both geological and development factors. Geological factors, such as reservoir heterogeneity, and development factors, such as development tools and processes, play a role [10, 14, 15]. However,

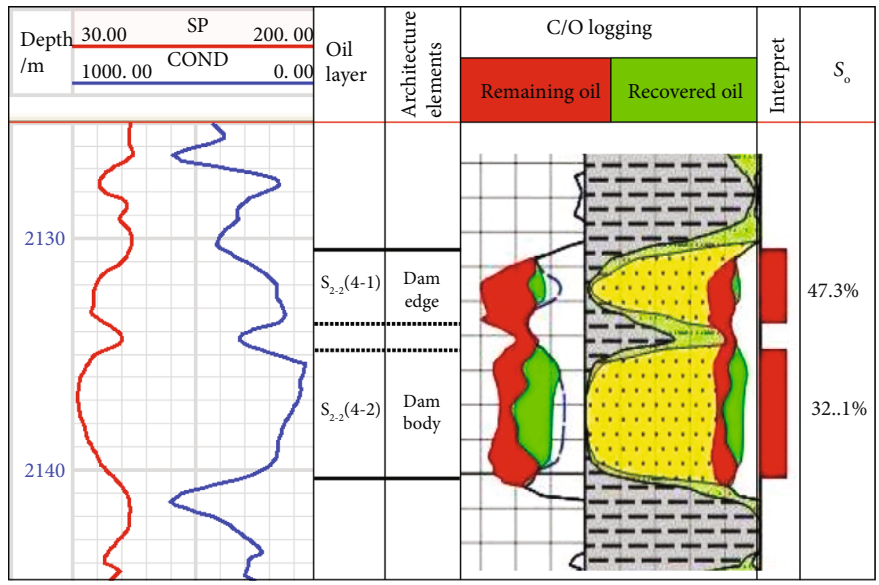

Figure 7: The column chart of well GN24-26 logging curves showing the architecture interpretation.

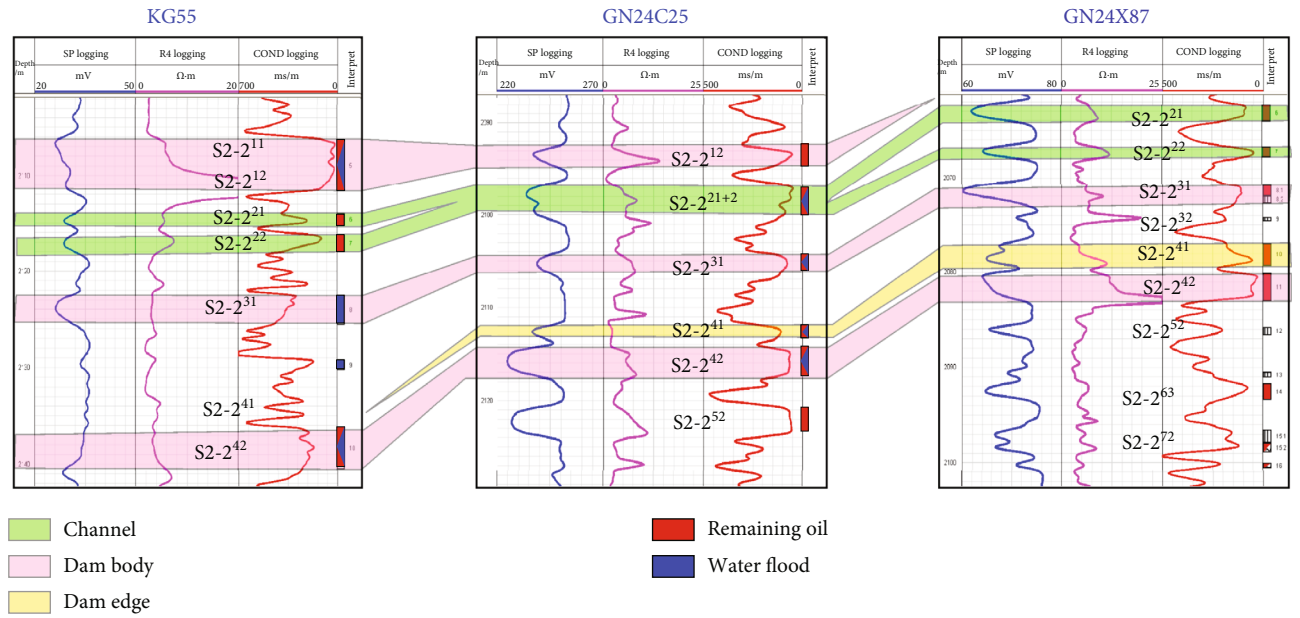

Figure 8: Profiles of S2-2 reservoir architecture element model across KG55-GN24C25-GN24X87 wells section in Hetan oilfield. As shown, the S2-2^{4} reservoir can be further divided into the main dam body layer (S2-2^{42}) which is the main oil production layer and dam edge layer (S2-2^{42}) which is the nonmain oil layer.

under certain geological and development conditions, the main influence on the distribution of remaining oil will shift to reservoir architecture and the difference in reservoir quality under its control [13]. The reservoirs of the estuary dam main body and the submerged diversion channel in the Hetan oilfield are of good quality and connectivity. The estuary dam's main body exhibits vertically reversed or homogeneous rhythmic characters. Due to the vertical difference in permeability and gravity divergence, the main reservoir of the injection and extraction linkage has a high degree of oil production development. However, it also suffers from severe waterflooded features, and the remaining oil is scattered and mixed in distribution. In the past, the development process focused mainly on the main reservoirs of the estuary dam main body or the submerged diversion channel, neglecting the recognition of the nonmain reservoir due to the constraints of a small oil-bearing area and the thin thickness of the nonmain reservoir. During the injection and production process of the main reservoir, the surrounding nonmain reservoir can be easily overtaken due to the difference in reservoir quality between the main reservoir of the dam body and the nonmain reservoir at the dam edge. As

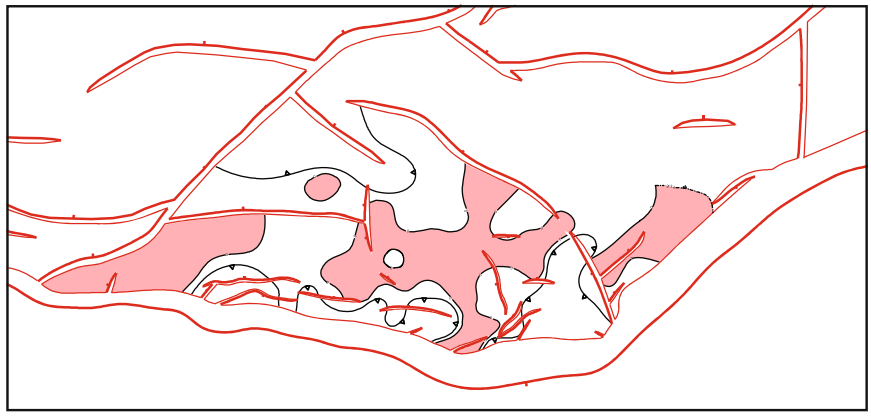

Fault
Denudation line
Layer region

(a)

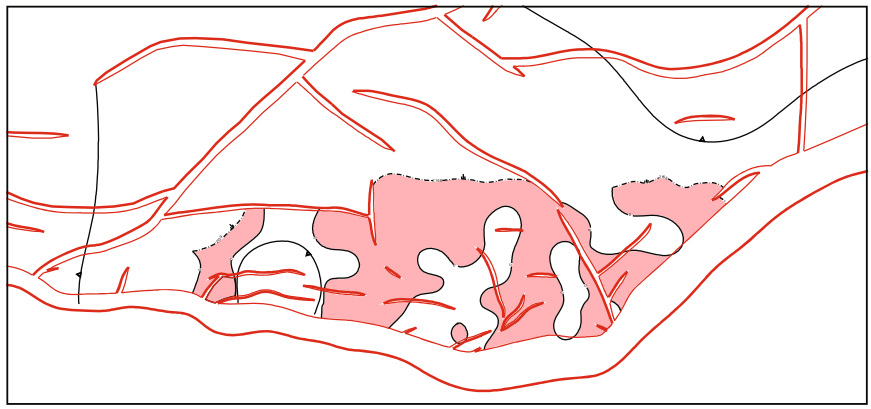

Fault
Denudation line
Layer region

(b)

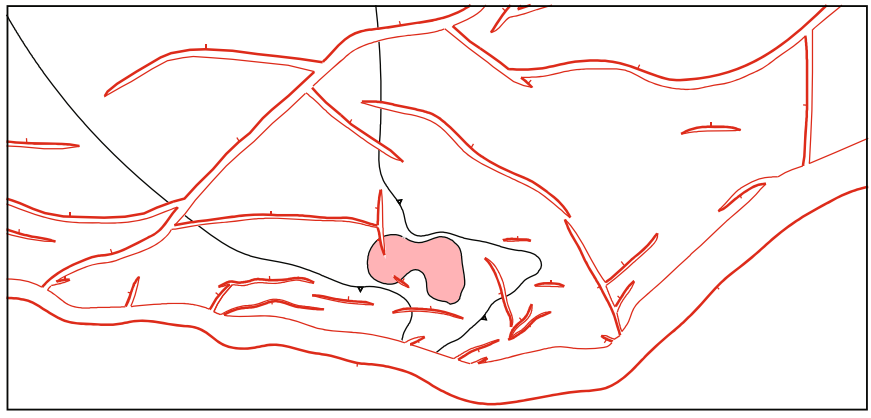

Fault
Denudation line
Layer region

(c)

Figure 9: Continued.

(d)

Figure 9: Plane distribution characteristics of nonmain reservoirs in the Hetan oilfield. (a) S2-2^{11} reservoir planar distribution with striped and fragmented shape. (b) S2-2^{41} reservoir planar distribution with striped and fragmented shape. (c) S2-2^{51} reservoir planar distribution with potato-shaped and only local distribution. (d) S2-2^{61} reservoir planar distribution with fragmented shapes.

Table 1: Statistics on the difference in reservoir quality of the nonmain reservoirs of S2-2 in the Hetan oilfield.

Reservoir	Area (km^2)	Thickness (m)	Average permeability (mD)	Coefficient of variation	Reserves ($\times 10^4$ t)
S2-2^{11}	0.8	2.8	726	0.82	21.8
S2-2^{23}	0.2	2.5	1054	0.86	4.9
S2-2^{32}	0.2	1.2	457	0.81	2.1
S2-2^{41}	1.0	1.5	527	0.71	19.2
S2-2^{71}	0.5	1.6	679	0.8	8.2
S2-2^{74}	0.3	1.2	820	0.8	4.7
S2-2^{75}	0.1	0.6	498	0.9	0.1
S2-2^{51}	0.1	1.4	388	0.8	2.4
S2-2^{52}	0.7	2.0	856	0.7	16.1
S2-2^{53}	0.5	1.8	1003	0.8	11.1
S2-2^{61}	0.4	1.4	465	0.9	7.3

a result, injection and production are ineffective in the nonmain reservoir at the dam edge, which has a low degree of waterflooded or is not waterflooded, leading to remaining oil enrichment. However, the nonmain reservoir on the dam edge has poor reservoir quality, making it challenging for injected water to penetrate the sand body during water injection and oil production. This results in a none or weak waterflooded features of the nonmain formation on the dam edge, leading to remaining oil enrichment and distribution. Therefore, even though the oil-bearing area of the nonmain reservoir at the dam margin is small, it still holds significant remaining oil reserves.

Based on the core description and saturation logging interpretation, the main oil layer of the Hetan oilfield exhibits medium-strong waterflooded features, high displacement efficiency, ratios of oil reserves in development, and recovery percentages of reserves. The nonmain reservoirs in the Hetan oilfield are estimated to contain a significant amount of remaining oil, with estimated reserves of approximately 1.42 million tons, accounting for 10% of the total reserves of the oilfield. However, the nonmain reservoir architecture imposes constraints, resulting in small oil-bearing areas for individual layers and overall limited remaining oil. For instance, the oil-bearing area of the nonmain reservoir S2-2^{11} is only 0.77 km^2 (Figure 9(a)), with a predicted reserve of approximately 220,000 tons. The oil-bearing area of the nonmain reservoir S2-2^{41} is 0.96 km^2 (Figure 9(b)), with a predicted reserve of nearly 200,000 tons. In contrast, the oil-bearing area of the nonmain reservoir S2-2^{51} is only 0.14 km^2 (Figure 9(c)), with a predicted reserve of about 25,000 tons. The oil-bearing area of the nonmain reservoir S2-2^{61} is 0.36 km^2 (Figure 9(d)), and the predicted reserves are about 73,000 tons. Therefore, the nonmain reservoir of the dam-edge architecture contains a certain scale of remaining oil enrichment due to the lack of direct injection and production correspondence. The reserves in the

nonmain reservoir can be better utilized through optimization and development method improvements.

4.3. Potential Digging of Nonmain Oil Layer and Field Application

4.3.1. Well Pattern Optimization Method. This paper presents a three-step optimization process for the new oil production well location and development of the nonmain reservoir in the Hetan oilfield. The geological characteristics of the oilfield, such as the scattered distribution of the nonmain reservoir, the large number of single-layer sand bodies, the small oil-bearing area, and the thin thickness of the oil layer, are taken into account. Additionally, the injection and production well pattern of the nonmain reservoir is missing, and the degree of reserve utilization is low with high remaining oil abundance. First, the minimum oil-bearing area required for the deployment of the new oil well is determined by calculating the limit well spacing. Due to the low permeability property of the nonmain oil layer, which is similar to the low-permeability reservoirs of Shengli Oilfield, the technical limiting well spacing is calculated using the limiting oil supply radius formula for low-permeability reservoirs in Shengli Oilfield [16]. The formula is as follows:

$$r = 3.226 \times (Pi - Pwfi) \times \left(\frac{K}{\mu}\right)^{0.5992}, \quad (1)$$

where r is the technical limit well spacing, m; Pi is the formation pressure, MPa; Pwfi is the bottom flow pressure of the well, MPa; K is the effective permeability, $\times 10^{-3}\,\mu m^2$; and μ is the viscosity of the subsurface crude oil, mPa·S.

The calculated results indicate that the technical limit well spacing is 210 m. Referring to the current effective well spacing used in the test field, a reasonable technical well spacing of 200 m is determined. Therefore, the minimum oil-bearing area for the deployment of the new well is determined to be $0.04\,km^2$.

Second, the minor oil layer screening was conducted, and a new well site proposal was designed based on the remaining oil area and predicted reserves of the nonmain reservoir sand body. The criteria for minor oil layer screening were established as follows: (1) the oil-bearing area of a single sand body should be $\geq 0.04\,km^2$, (2) geological reserves should be $\geq 1 \times 10^4$ t, and (3) the average effective thickness should be ≥ 1 m. Among the 47 nonmainstay single sand bodies, 22 potential sand bodies (accounting for 47%) with reserves of 117×10^4 t (accounting for 93%) and 25 nonpotential sand bodies (accounting for 53%) with reserves of 8.8×10^4 t (accounting for 7%) were screened out.

Finally, 22 sand bodies were identified and subjected to screening for potential. Well optimization was then carried out by designing multitarget wells. The plane projection and target positions of multitarget wells are illustrated in Figure 10(a), while the cross profile displaying target positions for each nonmain oil layer is shown in Figure 10(b). The design criteria for new wells were a single well control effective thickness of ≥ 5 m and control reserves of $\geq 5 \times 10^4$ t. The remaining 25 nonpotential sand bodies were either flexibly adjusted by drilling new oil wells in other oil layer development systems or by using old oil wells to change target layers. Following optimization, 76 new potential well targets were identified, along with seven new oil wells and two new water wells.

Due to the limited small oil-bearing area, thin reservoir thickness, and complex structure of the nonmain reservoir, the vector well pattern typically consists of a single-flow line or double-flow line. Continuous water injection is susceptible to water breakthroughs. In order to establish imitation marginal water flooding, it is important to flexibly adjust and exploit production potential through various means such as coupled water injection, periodic water injection, and suppressing strong and supporting weak water injection. This will lead to a more stable and effective production outcome. For instance, in the case of oil well GN24-55, the long flowline of well GN27-6 was utilized to maintain formation pressure. Additionally, well GN24-41 was used to establish a vector well pattern (Figure 11) and conduct periodic water injection to enhance the effectiveness of the water flooding. The results indicate that the water cut of the well GN24-55 was effectively controlled and production remained stable for seven years.

4.3.2. Field Application. The flexible injection and production development strategy proposed in this paper has been applied at the field site of the nonmain oil reservoir development in the Hetan oilfield. While simultaneously developing and adjusting the main oil layer, we consider the remaining oil enrichment and distribution characteristics of the nonmain oil layer. We use a series of screening and evaluation techniques for the nonmain oil layer and flexible injection and production adjustment studies to develop multitarget trajectory optimization for directional wells. The optimization and development of the nonmain oil layer were achieved by modifying the old wells and considering the reserve utilization of the nonmain layer in the new oil wells. Finally, a vector well pattern of flexible injection and production was established for the development of the nonmain oil layer in the Hetan oilfield.

The results of field application practice demonstrate that utilizing the flexible injection and production adjustment of nonmain oil layers maintains stable annual oil production and comprehensive water cuts in the oilfield. As of the end of 2021, the Hetan oilfield had achieved an oil recovery factor of 53.4%, with a recovery percentage of reserves of 59.8% and a maintained oil production rate of 0.62%. These results indicate high-quality, high-speed, and high-efficiency development. The development of the nonmain oil layer has improved the oil recovery factor of the entire Hetan oilfield from 43% to 53.4%, resulting in an incremental increase of over 10%. The natural decline rate over the past five years has remained within 7%, and the reservoir performance indicators of development have been positive. The effect of nonmain oil layer development is particularly significant. Using the nonmain oil layer of the S2 formation as an example, the cumulative effective thickness of the nonmain reservoir system in the S2 is over 200 m. The predicted remaining geological reserves of oil are about 1.25 million tons, with

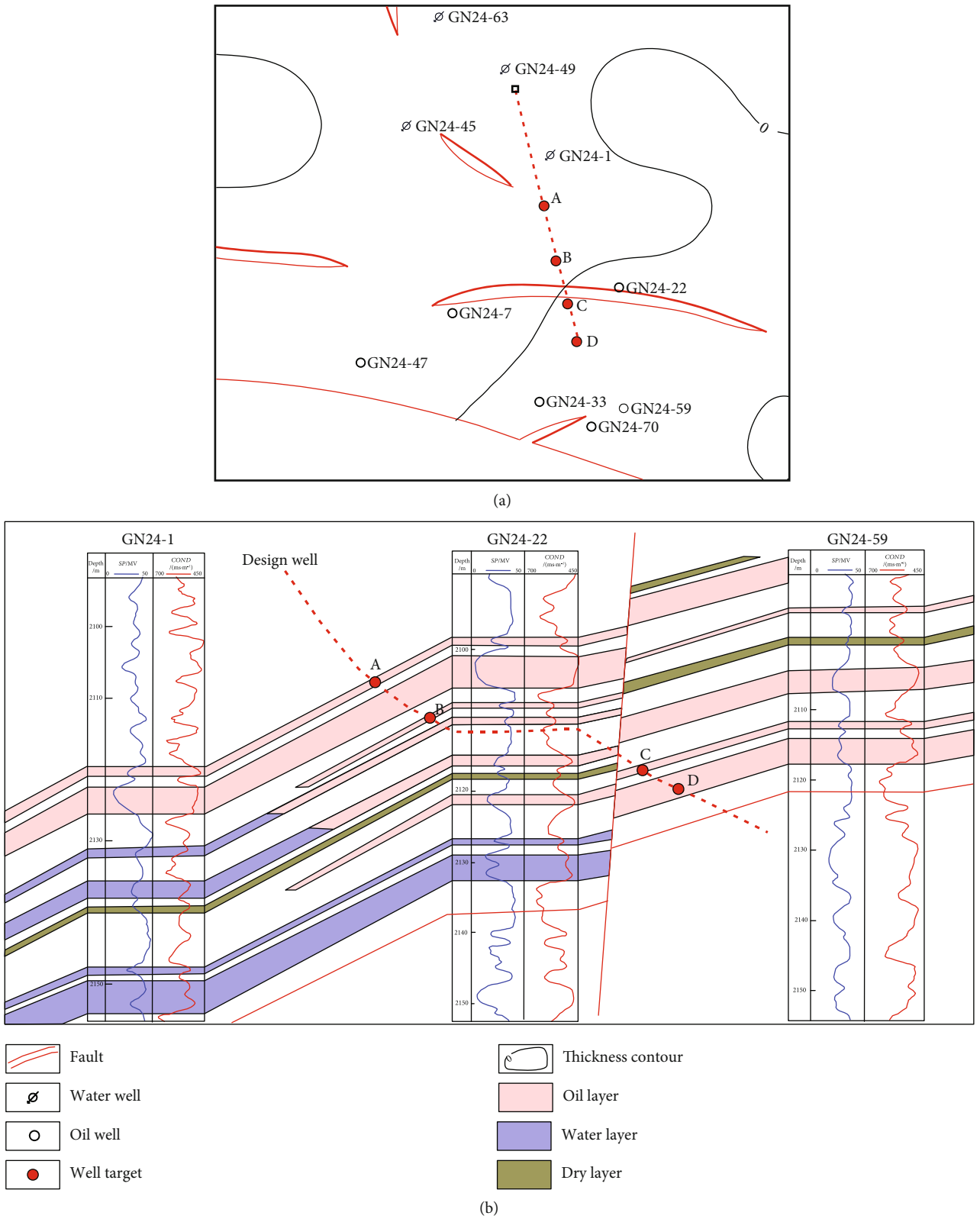

Figure 10: Multitarget well optimization model for the nonmain oil layer development in GN24-1-GN24-22-GN24-59 well profile in the Hetan oilfield. (a) New multitarget well track plane projection and targets position map. (b) New multitarget well track in well cross profile showing target position of each nonmain oil layer.

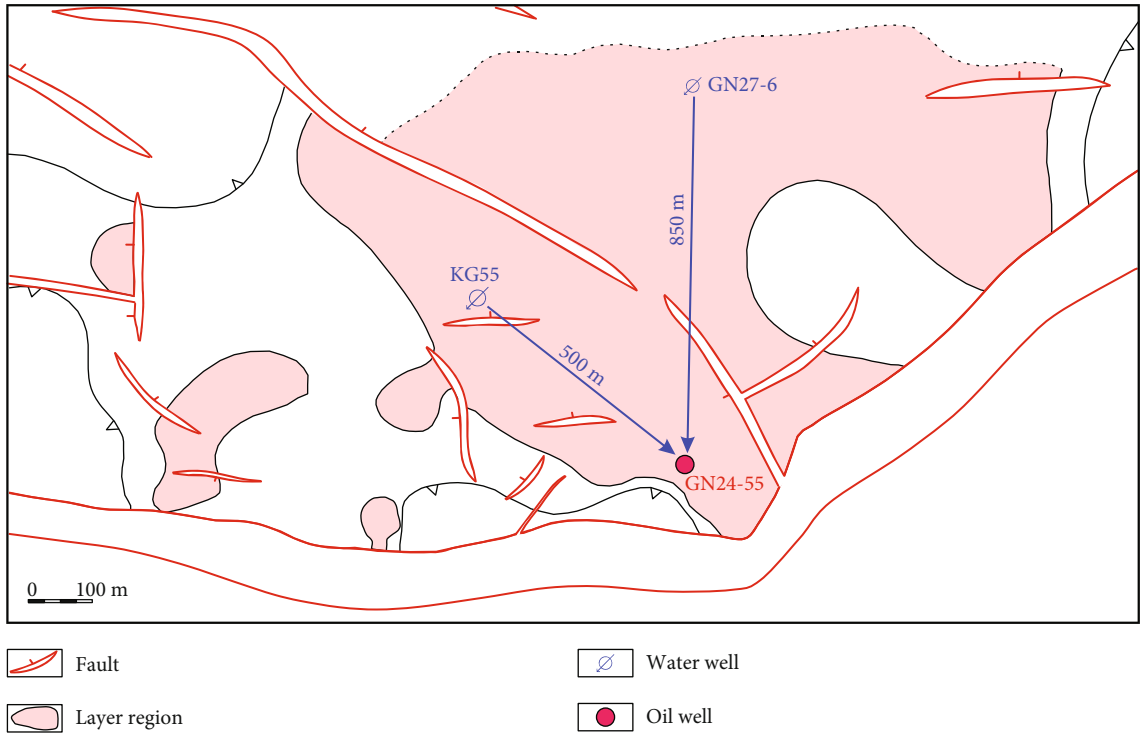

Figure 11: Diagram of the flexible adjustment of the well pattern in the nonmain reservoir of S2-1[32] showing an 850 m well spacing for ensuring formation pressure through a long flowline and a 500 m well spacing for vector well pattern.

only an 8.5% recovery percentage of reserves. By utilizing flexible injection and production adjustment methods, 7 new oil wells and 2 new water wells were drilled. Additionally, 6 old oil wells and 8 old water wells were reutilized, and 3 oil wells and 5 water well adjustment measures were taken. These actions resulted in the formation of a reasonable injection and production well pattern for the nonmain oil layer development of the S2 reservoir, as shown in Figure 12. After adjustment and optimization, the oil production capacity has increased to 12,000 tons, the water flooding control degree has reached 78.5%, the recoverable reserves controlled by a single well have reached 11,000 tons, and the oil recovery factor has increased from 16.7% to 28.5%, resulting in an increase of 11.8% in the oil recovery factor increment. It is worth noting that the best incremental oil recovery factors are found in nonmain oil layer developments.

5. Discussion

5.1. Sedimentary Model of Nonmain Reservoir. The microfacies map conventionally describes the distribution characteristics of composite sedimentary sand bodies in the plane, including submerged distributary channels, estuarine bars, and front sheet sand. However, this map may not fully reflect the heterogeneity of the reservoir. Utilizing a sedimentary model allows for a more accurate depiction of contact relationships and distribution characteristics of single-stage sedimentary sand bodies in the plane through the planar combination of sedimentary architecture elements. When studying nonmain oil layers, it is important to focus on the key contents, which are the fifth- and fourth-order architecture interfaces. The predelta mud layer between the estuarine bar and the distributary channel complex serves as the fifth-order architecture interface. The gamma-ray (GR) log curve is a baseline and effective interlayer due to its thickness and wide extension range. The fourth-order architecture interface serves as the physical interlayer between a single estuary bar or a single submerged distributary channel. This layer is typically composed of mudstone or silty mudstone and has poor physical properties that can impede fluid seepage in the sand body [7, 17]. As a result, the fourth- and fifth-order architecture elements usually form nonmain oil reservoirs with limited physical properties and local distribution.

The Gunan sub-sag, the location of the Hetan oilfield, is a remote deposit. Its source is primarily the Chenjiazhuang high in the south, along with two large braided river delta lobate deposits on the plane. The single submerged distributary channel is distributed in a strip on the plane, and its width is generally less than one well spacing (300 m). The single estuarine bar body is distributed in the shape of a lobe or ribbon, with an average width of 800~2000 m. The microfacies of the estuarine bar edge are situated at the boundary between the estuarine bar and the lacustrine mud. This results in the formation of nonmain oil reservoirs that are small, scatted, thin, and poor.

5.2. Controlling Factors of Remaining Oil Enrichment in Nonmain Reservoir. The distribution characteristics of the remaining oil in the high water cut period for the main reservoir of a thick sand body are mainly controlled by the blocking of different internal architecture element interfaces

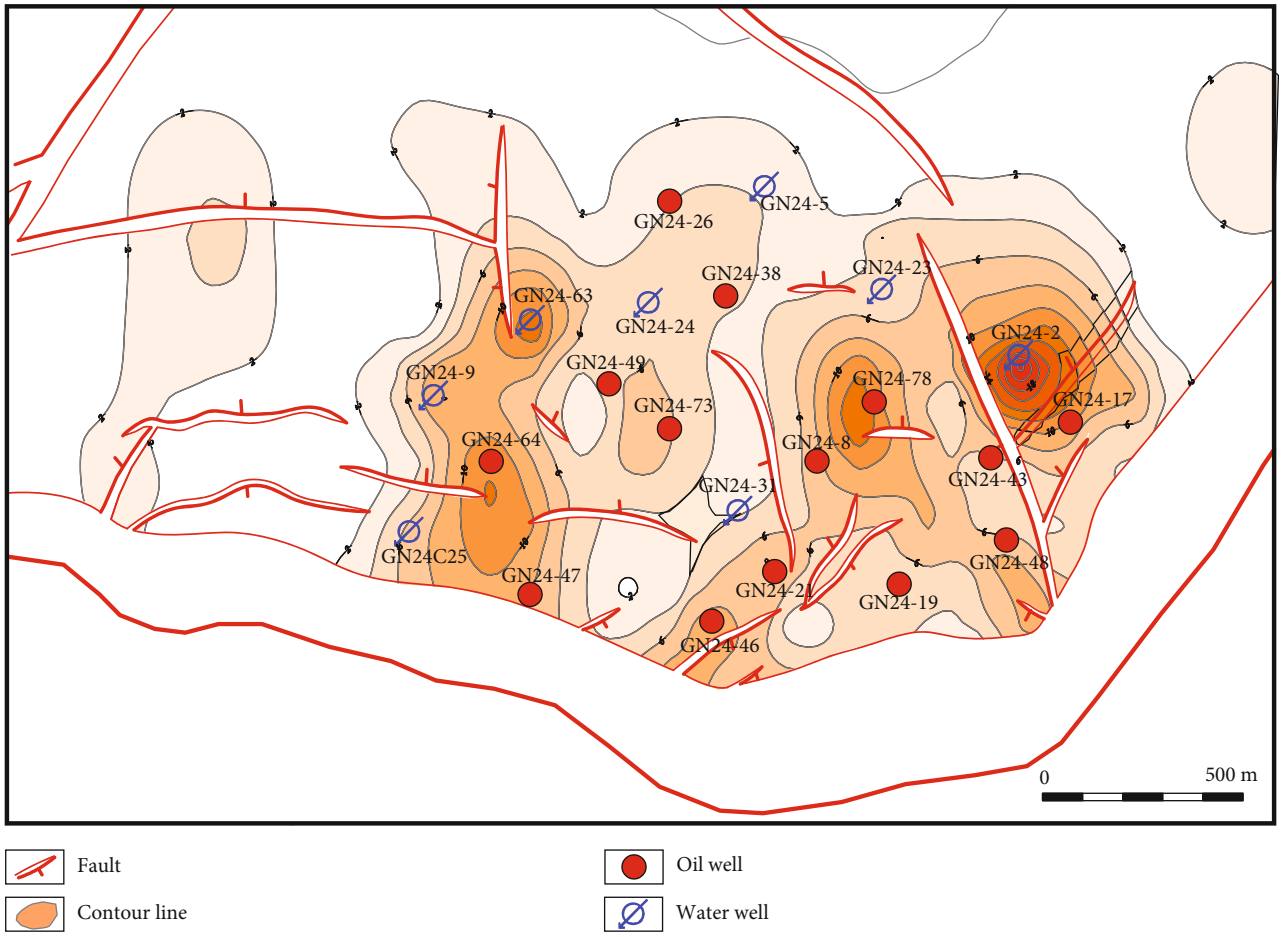

Figure 12: Effective thickness overlay contour line of the nonmain reservoir in the S2 formation and injection and production well pattern map. The cumulative effective thickness of the nonmain reservoir system in the S2 shows over 200 m, and the vector well pattern of nonmain oil layer development after the flexible injection and production adjustment and potential digging are also shown over the contour map.

(interlayers), in addition to gravity and deposition rhythm. These interfaces exhibit complex and diverse waterlogging characteristics such as bottom, middle, and top [10, 15]. However, the distribution of remaining oil in the thin nonmain layers is controlled by the seepage barrier and seepage difference of the accretion order architecture element in the single sand body. This is due to its relatively simple internal sedimentary structure. The inner interlayer of the estuarine dam is mainly composed of mudstone and silty mudstone, and it forms during the intermittent period of multistage growth. Therefore, the interlayer is mainly distributed in the progradation mode due to the progradation action of the estuarine bar [13]. The estuarine bar is divided into several independent accretions, causing lateral occlusion of the interlayer and resulting in uneven displacement of injection water, which leads to the enrichment of the remaining oil.

When the oilfield reaches the high water cut stage, the injection and production of the main oil reservoir are optimized, resulting in a high degree of reserve production. However, the injection and production of the nonmain oil reservoir have a relatively poor correlation, resulting in a low degree of reserve production and leaving a high amount of remaining oil reserves. During the high water cut period, a significant amount of remaining oil remains in the nonmain reservoir due to the combined influence of sedimentary architecture elements and plane injection-production relationships.

5.3. Optimization Processes of Improved Remaining Oil Recovery in Nonmain Reservoir. Improving production in small, scattered, and thin nonmain oil layers presents a significant challenge due to their unique characteristics. Accurately characterizing the distribution of the reservoir layer and remaining oil is necessary to flexibly adjust the remaining oil production plan of the nonmain oil layer when adjusting the main layers [9, 10]. Vector well patterns can be constructed by establishing multilayer perforating and horizontal wells and combining them with the secondary enrichment rule of remaining oil. Continuous optimization can be achieved through regular injection and production plan adjustments. The optimized well pattern should accurately focus on the distribution layer and location of remaining oil to continuously improve water drive efficiency.

To develop the remaining oil in nonmain oil layers, follow these feasible development, adjustment, and optimization processes. First, analyze the sedimentary architecture of the reservoir to accurately identify and divide the nonmain layers. Then, analyze the reservoir quality and heterogeneity of the nonmain layers and characterize the

distribution of remaining oil. Finally, the injection and production well pattern will be formulated based on distribution characteristics and the law of secondary enrichment of the remaining oil. The optimal well spacing will be determined, and the vector well pattern and production plan can be constructed to achieve the best development effect for enhanced oil recovery. Field tests have shown that this method greatly improves the understanding of reservoir and remaining oil distribution in nonmain layers. Targeted and flexible adjustment strategies can effectively improve oil recovery in nonmain oil reservoirs.

6. Conclusion

The nonmain oil layer is a crucial potential target for excavation during the late development stage of a complex fault block reservoir. Its significance lies in its ability to stabilize oil field production and expand capacity. This paper identifies the nonmain oil layers in the Hetan oilfield of Bohai Bay Basin, which are mainly deposited on the edge of the estuary dam, through the fine characterization of sedimentary microfacies and sedimentary architecture elements.

The lithology of the nonmain oil layers in the Hetan oilfield is primarily composed of gray and gray-white fine sandstone and siltstone, exhibiting parallel bedding and cross-bedding structures. The logging curves display funnel shapes and bell shapes, indicating sedimentary characteristics of multiple layers, small reserves, thin thickness, dispersed distribution, and poor physical properties. The reservoir thickness typically ranges from 1 to 3 m, with a permeability of less than 1 mD. The areas with favorable petrophysical properties were either banded, potato-shaped, or blocky. However, the connectivity between the injection and production planes was poor, with a coefficient of variation ranging from 0.71 to 0.9. The oil area of the single layer of the nonmain reservoir is small, ranging from 0.1 to 1.0 km^2, and the degree of waterflooded feature is low or nonexistent, resulting in a significant amount of remaining oil enrichment.

An efficient method for optimizing the trajectory of directional wells for multiple targets has been developed by using coupled water injection, periodic water injection, strength inhibition, and weakness reduction. The recovery factor of the nonmain oil layer increased from 16.7% to 28.5%, indicating successful development practices. By characterizing the reservoir more accurately and constructing flexible well patterns, the utilization of remaining oil in the relatively rich nonmain oil layers can be effectively improved.

The research and application tests in this paper demonstrate that for nonmain oil layers with relatively remaining oil enrichment, the utilization degree of remaining oil can be effectively improved by fine reservoir characterization and the construction of flexible development strategies of well patterns. This has important guiding and reference significance for the development of similar oilfields. However, to effectively address the development effectiveness of the nonmain oil layers, future work should focus on highlighting their development effectiveness and formulating an oilfield development program for these nonmain oil layers.

Data Availability

The data in this paper are from the actual geological data and oilfield development data of the Hetan oilfield of Shengli Oilfield Company of SINOPEC, China.

Conflicts of Interest

The authors declare no conflicts of interest.

Acknowledgments

This research was funded by the National Science and Technology Key Project of China "Tight Oil Development Demonstration Project in Bohai Bay Jiyang Depression" (No. 2017ZX05049-004). We would like to express our gratitude to the DeepL platform (https://www.deepl.com/write) for its assistance in the translation and editing process.

References

[1] Z. Li, W. Mei, L. Kong, and Q. Liang, "Countermeasures for reservoir adjustment and trapping the potential in Xingbei development area," *Journal of Oil and Gas Technology*, vol. 27, no. 1, pp. 228–230, 2005.

[2] C. Liu, Y. Chen, H. Wang, and J. Yang, "EOR for the oilfields in high water cut period," *Petroleum Geology And Recovery Efficiency*, vol. 8, no. 5, pp. 63–66, 2001.

[3] C. Wang, F. He, C. Liu, and W. Liu, "Research of fault-block reservoir at high water-cut stage to enhance development efficiency," *Fault-Block Oil & Gas Field*, vol. 11, no. 4, pp. 28-29, 2004.

[4] J. Jiang, E. Guo, Z. Wang, M. Zhai, X. Cao, and X. Zhang, "Study on potential exploitation measures of non-essential series of strata in Shuanghe oilfield," *Petroleum Geology And Engineering*, vol. 25, no. 4, pp. 87–90, 2011.

[5] Y. Li, X. Zhang, X. Sun, and Q. Meng, "Technique of tapping the potential of remaining oil at the late stage of high water-cut development in VIIIX oil formation of Shuanghe oilfield," *Journal of Oil and Gas Technology*, vol. 31, no. 5, pp. 152–156, 2009.

[6] L. Ma, Y. Qi, and E. Gao, "Fine geologic study on Bei III region and discuss on the residual oil distribution," *Petroleum Geology & Oilfield Development in Daqing*, vol. 19, no. 1, pp. 22–27, 2000.

[7] B. Tian, Z. Liu, C. Liu, X. Jia, and Y. Wang, "Configuration analysis and potential tapping practice of non-main reservoirs in SZ oilfield, Bohai Bay," *Journal of Xi'an Shiyou University (Natural Science Edition)*, vol. 34, no. 1, pp. 29–35, 2019.

[8] T. Gu, X. Zhang, S. Chen, and Q. Ma, "Further study on non-essential series of strata of mature exploration area: implication from tapping potential of Huangjindai oilfield," *China Petroleun Exploration*, vol. 12, no. 4, pp. 14–20, 2007.

[9] T. Zhang, "Research on improvement of oilfield development by effectively stimulating hon-payzones," *Special Oil and Gas Reservoirs*, vol. 22, no. 3, pp. 119–123, 2015.

[10] Y. Fang, E. Yang, S. Guo, C. Cui, and C. Zhou, "Study on micro remaining oil distribution of polymer flooding in class-II B oil layer of Daqing oilfield," *Energy*, vol. 254, no. 124479, pp. 1–11, 2022.

[11] X. Li, Y. Shi, L. Tang, and C. Yang, "Reconstruction of understanding system for the redevelopment in fault- block multilayer reservoir: case of Hetan oilfield in Zhanhua sag," *Acta Scientiarum Naturalium Universitatis Pekinensis*, vol. 49, no. 5, pp. 813–818, 2013.

[12] J. Wen, J. Liu, M. Qiao, and H. Zhou, "Sedimentary phase analysis of the Sha 3 reservoir in the Hetan oilfield," *Multiple Oil-gas Field*, vol. 3, no. 1, pp. 27–29, 2000.

[13] J. Li, P. Wang, B. Shang, C. Huo, and J. Xu, "Remaining oil distribution of delta front based on reservoir architecture: a case study of I oil formation of E_3d_2L in S oilfield, Bohai Bay Basin," *Fault-Block Oil & Gas Field*, vol. 26, no. 5, pp. 580–586, 2019.

[14] N. Liu, Q. Tang, J. Liu, J. Yu, Q. Li, and X. Hou, "Microscopic heterogeneity of Toutunhe Formation and its relationship with crucial short-term base level cycle in Fudong slope area, Junggar Basin," *Petroleum Geology & Experiment*, vol. 41, no. 2, pp. 234–242, 2019.

[15] G. Yan, Z. Liu, H. Song, X. Han, and X. Wang, "Remaining oil control factors and potential digging in offshore delta oilfield: taking JZ oilfield in Bohai Bay Basin as an example," *Fault-Block Oil & Gas Field*, vol. 25, no. 5, pp. 598–603, 2018.

[16] Y. Zhang, "Study on the reasonable well spacing of well pattern in block C274 of Dongfenggang oilfield," *Neijiang Science and Technology*, vol. 33, no. 12, pp. 155–157, 2012.

[17] S. Gao, S. Chen, H. Pu et al., "Fine characterization of large composite channel sandbody architecture and its control on remaining oil distribution: a case study of alkaline-surfactant-polymer (ASP) flooding test area in Xingshugang oilfield, China," *Journal of Petroleum Science and Engineering*, vol. 175, no. 1, pp. 363–374, 2019.